Experimental and analytical study of replaceable Buckling-Restrained Fuse-type (BRF) mild steel dissipaters

2013 NZSEE Conference

F. Sarti, T. Smith, A. Palermo, S. Pampanin

University of Canterbury, Christchurch, New Zealand.

D. Bonardi

Technical University of Milan, Italy

D.M. Carradine

Building Research Association of New Zealand, Judgeford, Porirua, New Zealand.

ABSTRACT: High-performance post-tensioned technologies for seismic resistance were first developed in the late 1990s as the main outcome of the PREcast Seismic Structural Systems programme (PRESSS). Of these technologies the hybrid connection, composed of the combination post-tensioning strands/bars (re-centring) and some form of mild steel element (hysteretic dissipation), was the most promising.
This paper focuses on the experimental study of a particular type of mild steel dissipation device: the fuse-type mild steel replaceable dissipater. This device is made up of a milled down plain mild steel bar and a confining tube filled with either epoxy or grout. The use of a milled area concentrates yielding over a defined length while the tube prevents buckling, similar to the Buckling Restrained Braces (BRB) used in steel frame buildings.
The main purpose of the experimental campaign was to provide a comprehensive parametric study and preliminary guidelines for the design of the replaceable device.
Several quasi-static push-pull tests were performed with varying geometric parameters such as the fuse diameter and length; two different filler materials were also used. Based on the experimental data collected, a simple analytical model was developed which is able to predict the force-displacement behaviour of the dissipater.

1 INTRODUCTION

High-performance post-tensioning systems were first proposed in the late 1990s as a main outcome of the PREcast Seismic Structural Systems (PRESSS) programme, coordinated by the University of California, San Diego. Different technologies were developed during the programme and tested on a five-storey building in the third and last phase of the experimental campaign (Priestley 1991). One of the outcomes of this body of research was the hybrid connection which combined re-centering (post-tensioning elements) and dissipative contributions (mild steel dissipaters) (Priestley et al. 1999).

As part of a series of experimental test campaigns performed at the University of Canterbury, a new external dissipation device, previously conceived by (Christopoulos et al. 2002) has been further developed, detailed and tested for both concrete and timber structural systems (Amaris et al. 2006; Palermo et al. 2006; Marriott et al. 2008; Smith et al. 2008). The dissipater is made of a mild steel bar machined down to a reduced diameter in order to concentrate yielding. To avoid buckling, the fuse area is encased in a steel tube which is filled with either grout or epoxy (Figure 1).

During two of these experimental campaigns (see Figure 2) characterisation testing has been performed on the stand-alone dissipative elements. Testing performed by Amaris Mesa (Amaris et al. 2006; Amaris Mesa 2010) included three different fuse diameters (7mm, 10mm, 13mm) with an unbonded length of 90mm. A 34mm diameter tube (2mm thick) filled with epoxy was used as anti-buckling restraint. The dissipaters showed stable hysteresis in tension, however in compression an increased stiffness was observed as well as buckling of the dissipater at relatively low displacements.

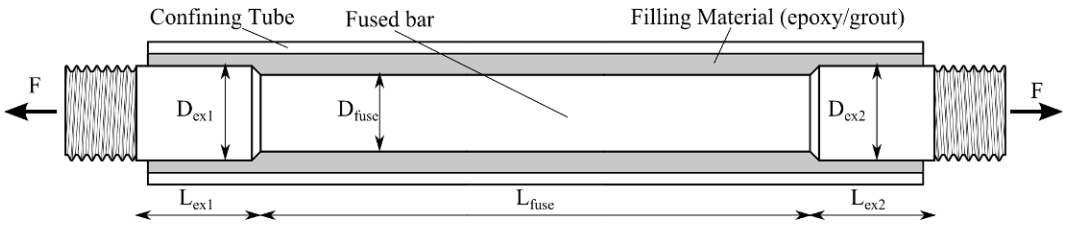

Figure 1. Buckling-restrained fuse-type (BRF) dissipater schematic and symbols

During the testing of Marriott (Marriott 2009), the dissipater elements were fabricated out of 20mm mild steel (Grade300) plain bars, with a reduced diameter of 10mm. The buckling restraining tube was 34mm in diameter (2mm thick) and filled with epoxy. Test results showed a very stable hysteresis and high energy dissipation capabilities (Marriott 2009).

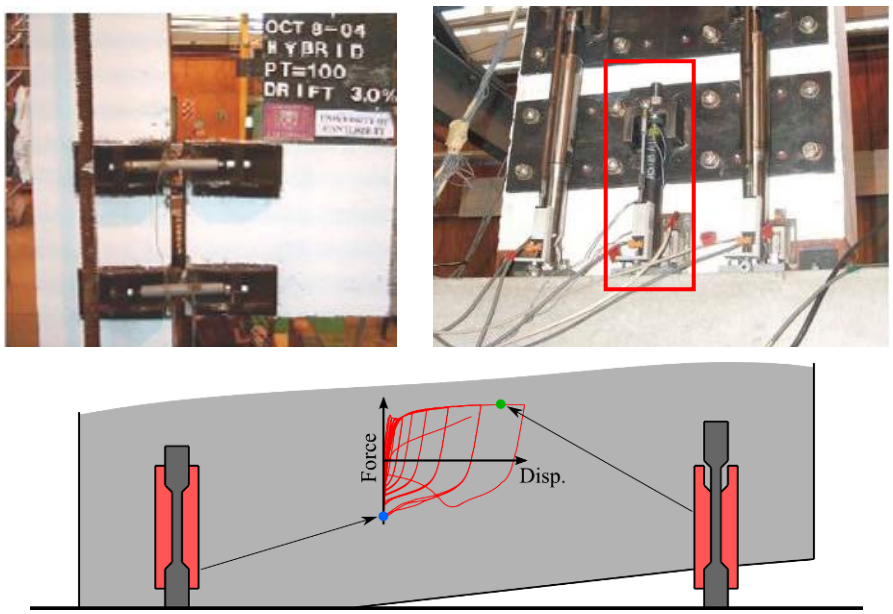

Figure 2. External dissipaters applications to beam-column joint (top left)(Amaris et al. 2006) and wall-foundation joint (top right)(Marriott et al. 2007). Detail of dissipater behaviour (bottom)

The fuse-type dissipation device has also been adopted for use in several buildings around New Zealand which have used post-tensioned technology. The first of these was the Learning and Research Building at Victoria University in Wellington (Figure 3 left). The building comprises of six three-bay concrete frames, spanning 8.4m, carrying double-tee flooring units spanning 9.9m. Energy dissipation was provided by external devices which were bolted to the pre-cast beams and columns after erection (Cattanach et al. 2008).

Figure 3. Beam column Joint real applications. Learning and Research building (left), Victoria University, Wellington (Cattanach et al. 2008), Merritt building (right), Christchurch

More recently a PRESSS multi-storey timber building, the Merritt building in Christchurch (Figure 3

right), has been designed and is currently under construction. The building is a three storey timber structure with post-tensioned frames spanning 8.8m in one direction. Fuse-type dissipaters are bolted at the beam-column and column-foundation interface to provide both dissipation and additional moment capacity.

The experimental campaign presented for this paper was carried out with the main objective of providing a comprehensive study into the performance of replaceable buckling-restrained dissipaters, and to develop and validate a simple analytical model capable of predicting dissipater behaviour.

2 EXPERIMENAL TESTING

2.1 Materials

Grade300 mild steel was used for both the fuse bars and the confining tubes. The filling material between the fuse bar and the tube was either cement grout or epoxy. Table 1 presents the characteristic properties of the materials used (provided by manufacturers).

2.2 Displacement protocol

The displacement protocol used during the testing was calculated in accordance with ITG-5.1-07 (ACI Innovation Task Group 5 2008). Each specimen was subjected to a sequence of positive quasi static (50mm/min) displacement-controlled cycles to pre-determined values as shown in Figure 4.

The compressive range of displacements was not accounted for because generally in all applications the compressive displacement is not significant in comparison to the tension displacement.

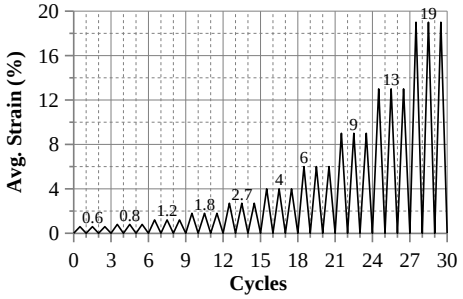

Figure 4. Loading protocol according to ITG-5.1-07

Table 1. Material properties

	Mild steel	Grout	Epoxy
Strength (MPa)	300	40	83
Young's Modulus (GPa)	200	30	1.5

2.3 Specimens and testing schedule

Different geometric parameters, (i.e. the plain/fuse diameters, the slenderness of the fuse bar) and the confining materials have been varied in order to provide a comprehensive set of experimental results from which design guidelines can be developed. For each configuration three specimens were tested (two grouted and one epoxied). A summary of the geometric properties is provided by Table 2.

Table 2. Testing schedule for buckling-restrained fuse-type (BRF) dissipaters (dimensions in mm)

ID No.	Plain diam. (D_{ex1})	Fuse diam. (D_{fuse})	Thread	Plain length (L_{ex})	Fuse length (L_{fuse})	Slender. ratio	Tube int. Diam.	Tube ext. Diam.	Tube length
D12L180	16	12	M16	40	180	60	21.7	26.9	256
D20L300	24	20	M24	40	300	60	36	42.4	377
D24L360	32	24	M30	40	360	60	40.3	48.3	440
D26L390	32	26	M30	40	390	60	40.3	48.3	468
D26L488	32	26	M30	40	488	75	40.3	48.3	566
D26L585	32	26	M30	40	585	90	40.3	48.3	665

Five different diameters have been chosen and slenderness ratio ($\lambda = 4L_{fuse}/d_{fuse}$) was taken into account as well; the majority of the specimens have been designed with a slenderness of 60, but for some a higher value has been considered ($\lambda = 75$ and $\lambda = 90$).

2.4 **Test setup**

Tests were performed using a Dartec displacement-controlled testing rig. Steel plates were fabricated in order to obtain the flexibility of test setup necessary due to the large range of dissipater size. Two large steel plates were bolted on the top and bottom of the testing machine to which smaller plates were bolted, the specimen was then screwed and bolted into this smaller plate. This setup allowed to the specimen to be easily replaced following testing. The test setup is shown in Figure 5.

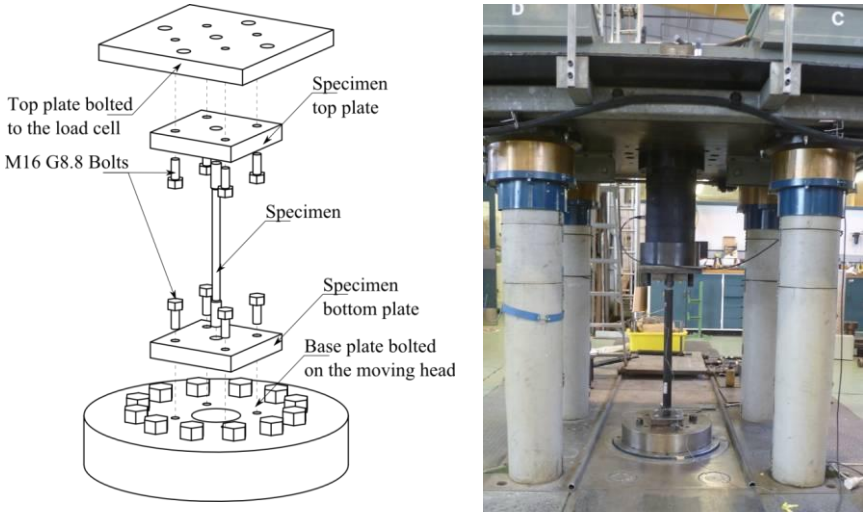

Figure 5. 3D exploded view (left) and picture (right) of test setup

2.5 **Results**

Results from tests performed are summarized in Figure 6, where the behaviour is reported in terms of force and displacement normalized by the specimen fuse length. A summary of the main parameters resulted from testing is reported in Table 3.

Table 3. Summary of test results

ID No.	Filler material	Slender. ratio		Max. Aver. Strain	Onset Avg. strain*	Ult. Avg. strain	Yield Force	Max. Compr. Force
		Fuse	*Dissipater*	*(%)*	*(%)*	*(%)*	*(kN)*	*(kN)*
	Grout			11.8		11.8	41.4	87.3
D12L180	Grout	60	37	8.8	-	4.5	42.3	94.8
	Epoxy			11.5		11.5	42.7	103.3
	Grout			12.8	12.8	6.7	97.7	232.8
D20L300	Grout	60	35	12.7	12.7	5.3	98.5	241.3
	Epoxy			8.9	8.9	7.2	95.4	182.5
	Grout			12.9	12.9	7.7	160.1	402.3
D24L360	Grout	60	36	12.9	12.9	12.9	160.2	364.8
	Epoxy			12.9	12.9	10.2	157.4	372.7
	Grout			8.9	8.9	6.9	207.0	360.0
D26L390	Grout	60	39	10.0	10.0	10.0	193.8	357.0
	Epoxy			12.9	12.9	8.0	208.0	305.3
D26L488	Grout	75	47	12.8	8.8	6.7	185.8	353.5
	Grout			8.9	8.9	10.4	185.6	307.2
	Grout			8.9	5.9	8.9	181.0	291.9
D26L585	Grout	90	55	11.5	5.8	11.5	187.5	293.0
	Epoxy			9.0	5.9	8.9	189.6	303.1

* maximum strain reached before the buckling mechanism of the dissipater occurred

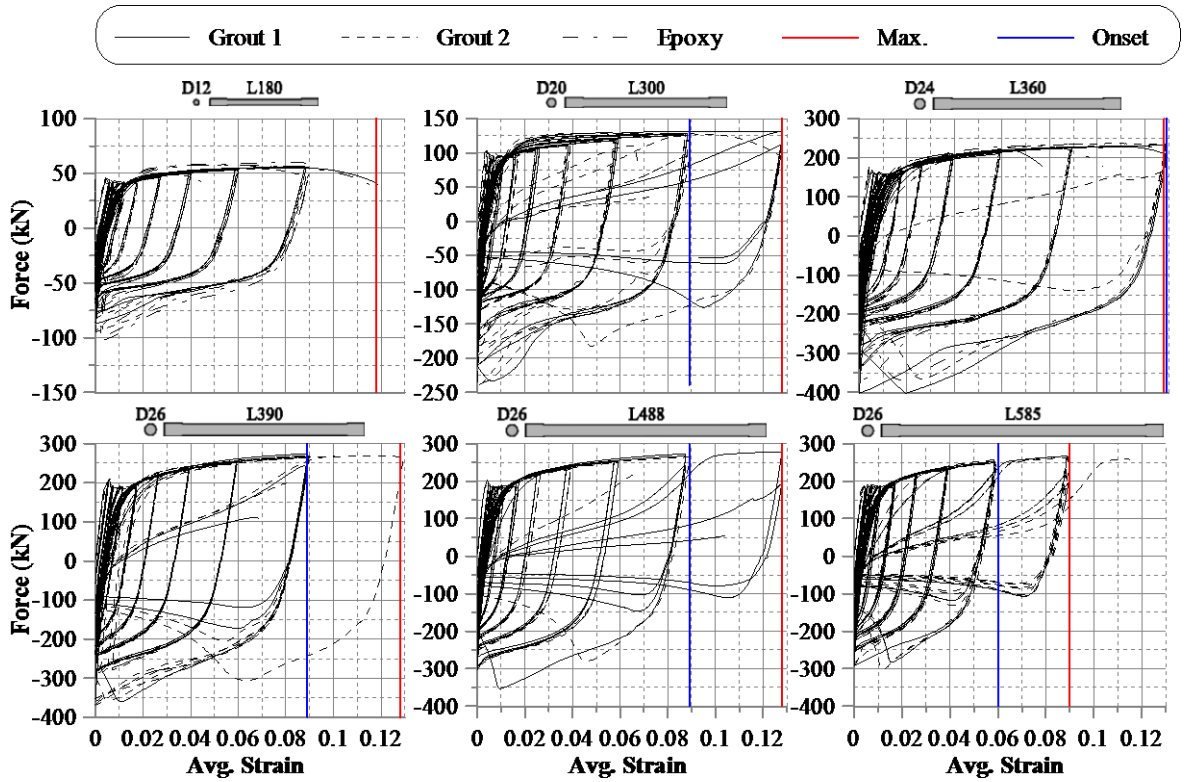

Figure 6. Force vs. normalized displacement chart of the tested dissipaters

The specimens with a slenderness value of 60 could undergo a normalized displacement of 9% before the dissipater started buckling. The buckling mechanism of the more slender specimens occurred on the reverse cycle at 9% and 6% (average onset strains in Table 3) for slenderness values of 75 and 90 respectively.

As Figure 6 shows, no major difference between the different materials used to fill the anti-buckling tubes was observed, with the dissipaters undergoing the same displacements, and onset at similar loads. The main differences in the use of either epoxy or grout as a filler material are in the ease of manufacturing and performance under high temperature. Epoxy is more fluid before hardening and is simple to pump into the cavity created by the anti-buckling tube. Epoxy does however have the disadvantage of degrading substantially when heated. This can occur during the tension compression cycles of the dissipater device as yielding of the material creates heat. Grout is less convenient from the constructability point of view, but its properties do not change significantly with increasing temperatures.

A minimum onset averaged strain of 6% up to a maximum value of 13% was observed. Onset strain is plotted in Figure 7 against the dissipater slenderness (i.e. the slenderness ratio of the composite section, see values in Table 3) and a linear trend was observed and plotted.

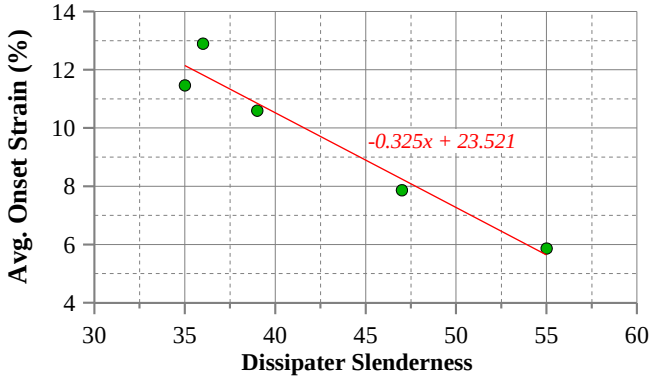

Figure 7. Onset strain vs. dissipater slenderness.

3 ANALYTICAL MODEL

The hysteretic behaviour of a post-tensioned system is reliant on the yielding in tension of the fuse-type dissipation devices. It is therefore crucial that the force-displacement characteristics of these elements are correctly predicted.

The analytical model presented is broken down into two main contributions: pre-yield and post-yield displacements. Both contributions are evaluated through the assemblage of three spring elements in series. Yield is limited to the fuse portion of the element.

3.1 Displacement contribution pre-yield

The yield displacement (Δ_y), considering yield to be isolated in the fuse area ($F = f_y A_{fuse}$) can be written as:

$$\Delta_y = \frac{f_y A_{fuse} L_{ex1}}{E A_{ex1}} + \frac{f_y A_{fuse} L_{fuse}}{E A_{fuse}} + \frac{f_y A_{fuse} L_{ex2}}{E A_{ex2}} \tag{1}$$

Where f_y is the steel yield stress. In most case $A_{ex1} = A_{ex2}$ therefore a single A_{ex} value will be used giving:

$$\Delta_y = \frac{f_y A_{fuse} (L_{ex1} + L_{ex2})}{E A_{ex}} + \frac{f_y L_{fuse}}{E} \tag{2}$$

A single value of the total external length ($L_{ex} = L_{ex1} + L_{ex2}$) will be used and given that $A_{fuse} = (\pi/4) d^2_{fuse}$ and $A_{ex} = (\pi/4) d^2_{ex}$ Δ_y can be rewritten as:

$$\Delta_y = \frac{f_y L_{fuse}}{E} \left(\left(\frac{d_{fuse}}{d_{ex}} \right)^2 \frac{L_{ex}}{L_{fuse}} + 1 \right) \tag{3}$$

This means that at yield a factor k_a can be defined in order to account for the additional displacement due to stresses in the areas between the anchorage of the dissipater and the fuse area:

$$\Delta_y = \frac{k_a f_y L_{fuse}}{E} \tag{4}$$

$$k_a = \left(\left(\frac{d_{fuse}}{d_{ex}} \right)^2 \frac{L_{ex}}{L_{fuse}} + 1 \right) \tag{5}$$

3.2 Displacement contribution post-yield

Considering an elastic-plastic stress-strain relationship, the strain of the steel beyond the yielding point (Δ) is:

$$\Delta = \Delta_y + \frac{\left(f_s - f_y \right) L_{fuse}}{E} \frac{1}{r} \tag{6}$$

Where r is the bi-linear post-yield stiffness factor and f_s is the steel stress, and the yield is assumed to be occurring in the fuse part only.

3.3 Discussion

As mentioned above, a complete understanding of the force-displacement relationship of the fuse-type dissipater is critical for incorporation within a post-tensioned system. Figure 8 shows a comparison between the procedure presented above and experimental results. A third line shows the force-displacement response when the fuse length only is considered (i.e. without the factor k_a)

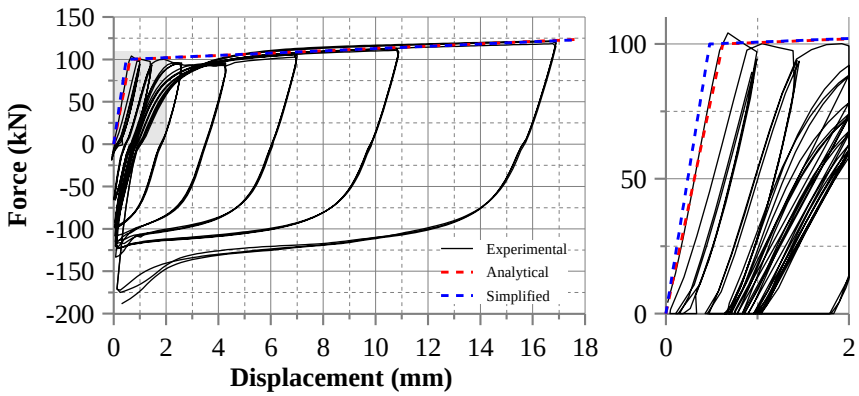

Figure 8. Experimental dissipater (D20L300) test results, the analytical model and the simplified assumption model comparisons

Using the analytical model proposed, the yield displacement of the dissipater D20L300 is evaluated as Δ_y = 0.62mm. Assuming the strain developing only in the fuse portion, the yield displacement of the dissipater would be $\Delta_y = F_y L/EA$ = 0.48mm. Comparison between these two yield displacement values and testing results shows that considering only fuse length (i.e. no k_a factor) significantly underestimates the yield displacement (by 23% in this example). No significant difference is observed in the post-yield behaviour.

4 ON GOING AND FUTURE RESEARCH

The research project on fuse-type dissipaters includes further numerical investigations. Finite element models will be calibrated on experimental data gathered during this study as well as data from an experimental database including previous tests performed at the University of Canterbury (Marriott 2009; Amaris Mesa 2010). The results will allow the calibration of a macro-model capable of capturing the general dissipater behaviour and its failure mechanisms.

5 CONCLUSIONS

A comprehensive parametric experimental campaign was presented in the paper. The different dissipaters tested showed stable hysteresis up to high level of displacements (9% average strain for most of the specimens). An experimentally calibrated linear relationship was worked out, relating the onset strain to the total slenderness of the specimen. This can be used for the evaluation of the maximum design displacement of dissipaters of this type.

Consistent results were observed with different filling materials (epoxy or cement grout), highlighting that this variable did not influence the behaviour of the devices.

An analytical model was developed to predict the behaviour of the dissipater and it was compared with the tests results. The experimental-analytical comparison showed the model could predict the yielding point as well as the post-yielding branch. Moreover, the model highlighted that for this dissipater type, the displacement contribution of the external parts cannot be neglected.

ACKNOWLEDGMENTS

The authors would like to acknowledge the Structural Timber Innovation Company (STIC) for funding this research.

REFERENCES

ACI Innovation Task Group 5 2008. *Acceptance criteria for special unbonded post-tensioned precast structural walls based on validation testing and commentary : an ACI standard*. Farmington Hills, Mich., American Concrete Institute.

Amaris, A., Pampanin, S., Palermo, A. 2006. Uni and bi-directional quasi static tests on alternative hybrid precast beam column joint subassemblies. *NZSEE Conference*, Napier, New Zealand.

Amaris Mesa, A.D. 2010. Developments of Advanced Solutions for Seismic Resisting Precast Concrete Frames. *Doctor of Philosophy*, University of Canterbury.

Bonardi, D. 2012. Analytical Modeling of the Cyclic Behaviour of a Replaceable Dissipater Device for Damage-Resisting Controlled Rocking System. *Master of Engineering*, Technical University of Milan.

Cattanach, A., Pampanin, S. 2008. 1st Century Precast: the Detailing and Manufacture of NZ's First Multi-Storey PRESSS-Building. *NZ Concrete Industry Conference*. Rotorua.

Christopoulos, C., Filiatrault, A., Uang, C.M., Folz, B. 2002. Post-tensioned Energy Dissipating Connections for Moment Resisting Steel Frames. *ASCE Journal of Structural Engineering* 128(9): 1111-1120.

Marriott, D., Pampanin, S., Bull, D.K., Palermo, A. 2007. Improving the Seismic Performance of Existing Reinforced Concrete Buildings using Advanced Rocking Wall Solutions. *NZSEE Conference*, Palmerston North, New Zealand.

Marriott, D.J. 2009. The Development of High-Performance Post-Tensioned Rocking Systems for the Seismic Design of Structures. *Doctor of Philosophy*, Universtiy of Canterbury.

Marriott, D.J., Pampanin, S., Bull, D., Palermo, A. 2008. Dynamic Testing of Precast, Post-Tensioned Rocking Wall Systems with Alternative Dissipating Solutions. *Bulletin of the New Zeland National Society for Eartquake Engineering* 41(2): 90-103.

New Zealand Concrete Society 2010. *PRESSS Design Handbook*.

Newcombe, M. 2007. Seismic design of multistorey post-tensioned timber buildings. *Master of Engineering*, Università degli Studi di Pavia.

Palermo, A., Pampanin, S., Fragiacomo, M., Buchanan, A.H., Deam, B. 2006. Innovative Seismic Solutions for Multi-Storey LVL Timber Buildings. *9th World Conference on Timber Engineering*. Portland, Oregon, USA.

Priestley, M.J.N. 1991. Overview of PRESSS research program. *PCI Journal* 36(4): 50-57.

Priestley, M.J.N., Sritharan, S., Conley, J.R., Pampanin, S. 1999. Preliminary Results and Conclusions from the PRESSS Five-Story Precast Concrete Test Building. *PCI Journal* 44.

Smith, T., Pampanin, S., Buchanan, A.H., Fragiacomo, M. 2008. Feasibility and Detailing of Post-tensioned Timber Buildings for Seismic Areas. *New Zealand Society of Earthquake Engineering, Annual Conference*, Wairakei, New Zealand.

STIC. http://www.stic.co.nz